Mechanism for Mechanical Wave Break in the Heart Muscle

L. D. Weise[1,2] and A. V. Panfilov[1]
[1]Department of Physics and Astronomy, Ghent University, Krijgslaan 281, S9, Ghent 9000, Belgium
[2]Theoretical Biology, Utrecht University, Padualaan 8, Utrecht 3584 CH, Netherlands
(Received 2 March 2016; revised manuscript received 8 June 2017; published 7 September 2017)

Using a reaction-diffusion-mechanics model we identify a mechanism for mechanical wave break in the heart muscle. For a wide range of strengths and durations an external mechanical load causes wave front dissipation leading to formation and breakup of spiral waves. We explain the mechanism, and discuss under which conditions it can cause or abolish cardiac arrhythmias.

DOI: 10.1103/PhysRevLett.119.108101

Spiral waves were observed in various excitable media, e.g., the Belousov-Zhabotinski (BZ) reactions [1,2], in nerve tissue where they underly neurological diseases [3], and during morphogenesis of a slime mold [4,5]. In the heart spiral waves of electrical excitation can cause life-threatening cardiac arrhythmias [6].

Electrical activity of the heart governs its mechanical pumping [7]. However, also its deformation affects its excitation processes. This "mechano-electrical-feedback" (MEF) has been shown to be able to cause, but also to abolish, cardiac arrhythmias e.g., due to mechanical impact on the chest [8,9]. However, the basic mechanisms of mechanical wave break are poorly understood. To study the effect of MEF on excitation waves, coupled reaction-diffusion-mechanics (RDM) models were introduced [10–12].

Here we apply a RDM model [13] to identify a mechanism of wave break which connects MEF to the phenomenon of wave front dissipation [14].

Our method [13] couples a model for human cardiac cells [15], with a discrete mechanical model for cardiac tissue [12], and a model for excitation-contraction coupling [16,17] adjusted to human cardiac tissue [18]. Nonlinear waves of electrical excitation are modeled via a reaction-diffusion equation for the transmembrane potential V

$$\frac{\partial V}{\partial t} = D\Delta V - \frac{I_{\mathrm{ion}} + I_{\mathrm{sac}}}{C_m}, \tag{1}$$

with membrane capacitance density $C_m = 2.0\ \mu\mathrm{F/cm^2}$ and diffusivity $D_{ij} = \delta_{ij} \times 0.00154\ \mathrm{cm^2/ms}$. Transmembrane ion current I_{ion} is modeled by time- and voltage-dependent ion channels [15,19]. The finite difference mesh for the explicit Euler integration [20] of Eq. (1) is coupled to a square lattice of mass points connected with springs (see Fig. 1 in [13]). Excitation waves trigger contraction [13]. To solve the mechanical model we assumed elastostatics, and used Verlet integration [21]; compared to our previous work [13] we used different parameters [22]. To model MEF we use a linear, time-independent model for stretch-activated currents (I_{sac})

$$I_{\mathrm{sac}} = G_s \frac{(\lambda - 1)}{(\lambda_{\max} - 1)}(V - E_s), \quad \text{for } \lambda > 1 \tag{2}$$

where λ is the normalized sarcomere length in one-dimensional (1D) simulations, and the square root of the normalized area of a quadrilateral formed by direct neighboring mass points (see Fig. 1 in [13]) in two-dimensional (2D) simulations. We chose maximal value $\lambda_{\max} = 1.1$ [13]. G_s is maximal conductance, and E_s is the reversal potential. E_s ranges from -20 to 0 mV according to different sources [23,24]; we set $E_s = 0$ mV. For G_s a range within 0–100 S/F has been reported [9,25], and we use $G_s = 100$ S/F for 2D simulations, and vary it in 1D simulations.

For 2D simulations we used a square medium with side length 20 cm, where points of the upper edge were held fixed in space and points at side edges were allowed to move up- and downward. An external mechanical load was applied to lower border points of the model (Fig. 1). We can relate our model to a thin slice of cardiac tissue with a constant thickness, in which pressure p is applied to the surface of one side. Corresponding forces acting on mass points at the lower edge are $\vec{f}_i = pS_m\vec{n}$, where $\vec{n}$ is the normal vector, and $S_m = 0.025\ \mathrm{mm^2}$ is the mass point area spread of the undeformed mesh. We considered two scenarios. In the setup "point source" waves were initiated at the left, upper corner with a period of 333 ms. It resembles a condition when a point source of excitation causes a rapid heartbeat. In the other setup, "spiral wave," a spiral wave is present. It resembles a state of cardiac tachycardia when a spiral wave source causes a rapid heartbeat. It is important, because a breakup of a spiral wave is considered as a mechanism of transition from tachycardia to fibrillation leading to sudden cardiac death [26]. For initial preparation we performed simulations at an isotonic load ("normal load") of 5 kPa for 7.686 s for the point stimulation setup, and 6 s for the spiral wave setup. After that a pulse of external mechanical load with a certain maximal "strength" and "duration" was applied. The external mechanical load is increased within 20 ms to its maximal strength, and after a certain duration, decreased

back to normal load within 20 ms. We varied the main parameters strength and duration of the applied external mechanical load.

For 1D simulations we used a 20 cm long cable stretched to $\lambda = \lambda_{\max}$. To alter I_{sac} in the cable we vary G_s in Eq. (2). We prepared the cable for 6 s by starting waves at one end with 2 Hz for a certain strength of I_{sac}. After this preparation we performed further experiments.

We found that the external mechanical load causes a wave break (Fig. 1). We found two generic regimes of wave break formation present in both setups [27]. In regime **I** wave break occurs when a short strong stretch is applied (Fig. 1, upper panel). In regime **II** wave break occurs after a release of a long external load (Fig. 1, lower panel). In Fig. 1, upper panel (0, 34, and 68 ms) we see how a strong stretch increases conduction velocity (CV), while the velocity of a wave back seems to be not affected [28]. As a result a wave front collides with the wave back of the preceding wave, breaks, and forms a spiral wave [Figs. 1, upper panel (68, 178, and 838 ms)]. In Fig. 1, lower panel we see that a release of a long external load causes an increase of CV (280, 468, and 516 ms) while the wave back velocity seems to be not affected. Again, wave front-back collision produces a wave break, leading to new spirals [Fig. 1, lower panel (606 and 890 ms)].

In both regimes wave break occurs due to an increase of CV. However, in regime **I** we see that this increase occurs shortly after the start of stretch, while in **II** it occurs after a release from a long stretch. The effect of strain on CV has been studied before, experimentally and theoretically (see reviews: [29–31]). However, little is known about the direct response of CV on a change in strain. To study how external stretch affects CV via I_{sac} we applied the 1D setup [32]. From Fig. 2(a) we see that the immediate reaction of a wave to stretch is an increase of CV. A further increase in I_{sac} (compare G_s in inset) amplifies this effect. This can be explained by the increase in resting potential due to activation of I_{sac} [33], which reduces the transmembrane potential and brings it closer to the threshold of the action potential generation [13]. However, for stretch longer than ≈25 ms another effect takes place which causes wave slowing. For $G_s < 25$ S/F, CV decreases to slower values compared to not-stretched medium (black line). For $G_s \leq 20$ S/F and duration of external stretch > 25 ms, CV monotonically decreases and converges to constant "normal CV" which is smaller for higher values of G_s. This is due to the accommodation effect—a decrease in sodium channel availability due to depolarizing I_{sac} [13,34]. For higher I_{sac} [see lines corresponding to $G_s > 24$ S/F in Fig. 2(a)] another phenomenon occurs—a transition to a "phase wave." A phase wave can travel infinitely fast, because it is not propagating by diffusion but a shift of phase [35]. Here a shift of phase in excitation is due to the stretching of the medium. CV diverges due to simultaneous excitation of the cable by I_{sac}.

Figure 2(b) illustrates the effect of release of stretch on CV. The immediate response of a wave to a release of stretch is an abrupt decrease in CV. The effect is higher for larger G_s. This slowing is because the release of stretch causes a decrease in I_{sac} which decreases the transmembrane potential [13]. This slowing effect is most pronounced ≈25 ms after stretch release, when CV is minimal. For time > 25 ms after stretch release, we see that the wave accelerates until CV converges to the normal CV in a not-stretched medium. Note that these effects on CV do not immediately affect the velocity of a wave back ahead of the propagating wave, because the wave back mainly follows the time course of the action potential initiated by the previous wave front. Thus, a change of stretch promotes wave front-back collision.

Why and under which conditions does such a collision lead to wave break? To understand this we refer to the phenomenon of wave front dissipation which was first characterized and studied by Biktashev in a series of papers [14,36,37]. Dissipation means that a wave front will halt, if it is forced to propagate slower than a certain "critical CV" [14]. The mechanism for this conduction block is connected to the accommodation of the cells—a weak

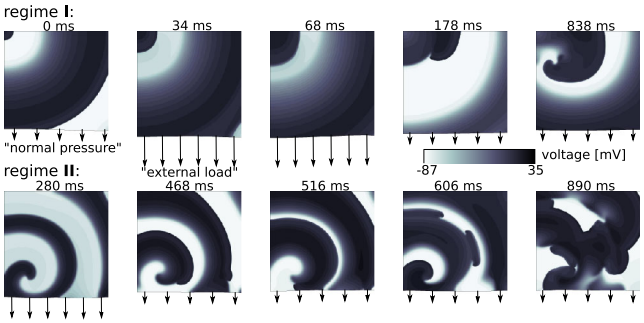

FIG. 1. Pulse of external mechanical load causes wave break. Upper panel—regime **I**: wave break is caused by a short pulse (50 ms, 23.5 kPa). Lower panel—regime **II**: wave break is caused by release of a long pulse (350 ms, 17.0 kPa). Arrows symbolize applied external stretch.

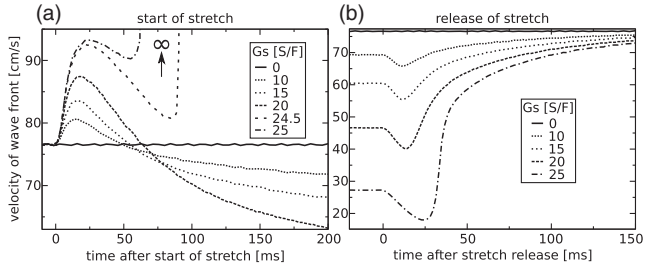

FIG. 2. CV vs stretch. (a) Stretch application. A wave is initialized at one end of the unstretched fiber at time 7 s, constant stretch ($\lambda = \lambda_{\max}$) is applied 50 ms later for different G_s. (b) Release of stretch. The fiber is held stretched for different G_s, at time 7 s a wave is initialized at one end of the fiber, 1.0 s later stretch is released ($\lambda = 0$). 6 s prior experiments' waves were started at one end of the fiber with 2 Hz for different G_s.

depolarizing current increases the minimal diastolic potential which inactivates fast sodium channels and increases their reactivation time before an action potential is triggered [19,38,39]. In the case of dissipation, diffusive currents cause a slow depolarization in forward direction of a wave and thus accommodation. To show that wave front dissipation is connected to our results we studied the critical CV of a wave front interacting with a wave back, and how this is affected by I_{sac}. We used the setup illustrated in Fig. 3(a). To determine the critical CV, we introduced a moving inexcitable block in a cable of cardiac tissue which forces wave S1 to a certain velocity. As we are interested in the dissipation of a wave front at the tail of the previous propagating wave we initiated a wave S2 which interacts with the wave back of S1. The wave S2 was initiated in the cable 0.5 s after wave S1. Wave S2 initially propagated faster than wave S1 until it interacted with the wave back of wave S1, and either continued propagating at the forced CV, or dissipated. Figure 3(a) illustrates the setup of inexcitable block, S1 wave, and S2 wave.

Figure 3(b) illustrates the process of dissipation of a wave (S2) at the back of a preceding wave (S1). We see from the upper panel of Fig. 3(b) that the upstroke of S2 is increasingly hindered for slower forced CV. From the lower panel we see that the hindered upstroke is due to the deactivation of sodium channels in front of the wave.

Figure 3(c) shows the critical CV (minimal forced CV when propagation of wave S2 was still possible) as a function of G_s. The critical CV is substantially lower than

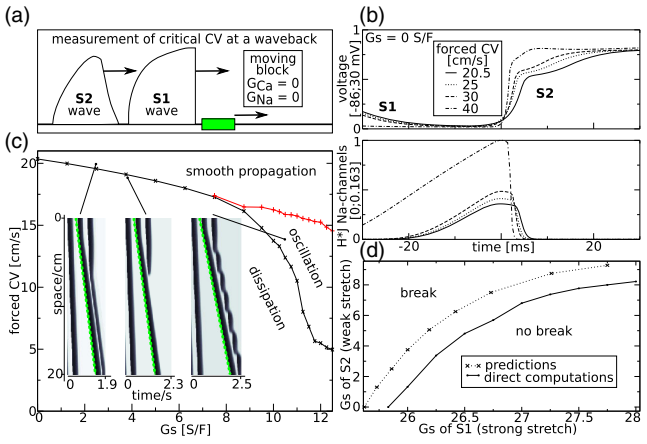

FIG. 3. Wave front dissipation at a wave back vs I_{sac}. (a) Setup: moving inexcitable block (rectangle) in a cable of cardiac tissue (line) forces wave S1 to propagate at "forced CV." Wave S2 is interacting with the wave back of S1. (b) S2 wave front dissipation at wave back S1. Upstroke shape (upper panel) and sodium channel availability (lower panel) of S2 waves vs time for different forced CV values. Time was shifted for different simulations so that maximal availability of sodium channels is at 0 s. (c) Regimes of S2 propagation vs forced CV and G_s. Insets: time space plots; dotted lines illustrate moving block. (d) Prediction of border to wave break after a release of stretch using critical and normal CV vs direct computations.

the normal propagation speed (compare Fig. 2). Indeed for $G_s = 0$ the normal CV is 74.0 cm/s (Fig. 2) while the critical CV is 20.4 cm/s. In general, we find that the critical CV is ≈3.5 times lower than normal CV. With an increase of G_s the critical CV gradually decreases. This is because I_{sac} supports the upstroke of the wave S2. However, for higher I_{sac} ($G_s > 7.5$ S/F) the wave front propagation becomes nonmonotonic: the wave slows, partially dissipates, then it recovers, and again collides with the S1 wave back. We refer to this as oscillation regime, because wave propagation oscillates between normal and slow conduction. We can understand this as a manifestation of biexcitability of cardiac tissue [40,41]. A depolarizing current (here I_{sac}) can promote a calcium-driven upstroke, when sodium channels are deactivated [40].

We use the critical CV [Fig. 3(b)] and the normal CV vs I_{sac} (Fig. 2) to predict which stretch release will cause wave break in the 1D system via regime **II** [42]. For direct computations we consider propagation of the S1 wave at a constant, strong stretch (G_s at horizontal axis), and then abruptly release stretch (100 ms after upstroke of S1) to a constant, weaker stretch (G_s at vertical axis). The main idea is that if the critical CV of the S2 wave is slower than the CV of wave S1 it will result in the dissipation of the S2 wave after colliding with the back of the S1 wave. The dependencies for normal and critical CV can be used to predict when a stretch release will result in wave break [43]. Figure 3(d) shows that the predicted values are reasonably close to the values obtained by a direct computation with a relative error of about 2%.

We found that our mechanism occurs in both setups for a wide range of parameters strength and duration of an external mechanical load [colored dots in Figs. 4(a) and 4(b)]. Regime **II** does not occur in both setups for a stretch duration shorter than 100 ms. Wave break in the point source setup occurs most often via regime **I**, whereas in the spiral wave setup it is most often via regime **II**. In the point source setup regime **II** requires in most cases the application of a weaker, but longer mechanical stimulus, compared to regime **I**. However, in the spiral wave setup

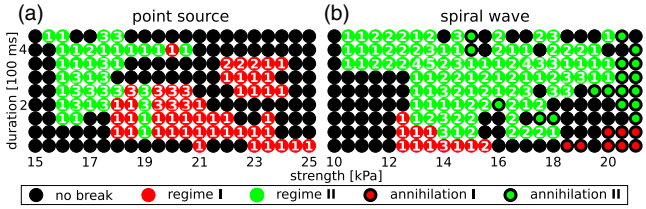

FIG. 4. Wave break in 2D model vs strength, duration of stretch. Dots indicate outcomes for individual simulations. Colored: wave break causes or annihilates spirals—red: regime **I**; green: regime **II**. Ciphers: number of new spiral wave sources 0.5 s after release of stretch. Black contours: annihilation of spiral wave. Black dots: no formation or annihilation of spiral waves. (a) Point source setup. (b) Spiral wave setup.

regime **II** occurs for a wide range of strength, and regime **I** between [12.5; 15.5] kPa. In the spiral wave setup regime **I** occurs for stretch durations shorter than 200 ms. However, in the point source setup, it can happen also for longer stretch durations. In the spiral wave setup a weaker mechanical stimulus is required: for the spiral wave setup 10 kPa is the smallest strength to result in wave break, compared to 15.5 kPa in the point source setup.

We found stretch ≥ 15 kPa can cause spiral wave annihilation via both regimes [see colored dots with black contours in Fig. 4(b)] [44]. Also mechanical load causes wave front-back collision and wave break; however, no spiral wave source remains in the medium. We see from Fig. 4(b) that a spiral annihilation is more likely the stronger and longer a pulse is applied. In the point source setup, waves were started with a rapid pacing frequency of ≈3 Hz. However, the normal heart rate is around 1–2 Hz. For a lower heart rate, waves are more distant to each other, and it seems unlikely that our mechanism can result in spiral wave initiation. However, we can still obtain spiral formation via regime **I**, because a strong stretch can induce a new wave via MEF [9,33]. We illustrate it in Fig. 5 [45]. Figure 5 shows that a short, strong stretch induces a new wave (26 ms), that propagates very fast (phase wave) and collides with a wave back (50 ms). The wave breaks (206 ms), and a spiral wave forms (614 ms).

For the latter case the vulnerable window for our mechanism is given by a simple requirement that a wave back is present in the medium, and the medium behind it is excitable. However, when the applied mechanical load does not produce a new wave, we need to discuss the effect of the system size to understand its impact on the onset of cardiac arrhythmias. As this mechanism requires a wave front-back collision we find [46] that the minimal system size $d_{\min}$ [in 1D, compare Fig. 3(a)] necessary for collisions is

$$d_{\min} = \frac{\mathrm{CV}_f \times \mathrm{CV}_s}{\mathrm{CV}_f - \mathrm{CV}_s} \times (T - \mathrm{APD}), \tag{3}$$

where CV_f is CV of the faster wave, CV_s of the slower preceding wave, T period of stimulation, and APD is the action potential duration. A front-back collision of waves will thus happen if $T < \mathrm{APD} + d_{\min}/\mathrm{CV}_s - d_{\min}/\mathrm{CV}_f$. Assuming for the heart muscle $d_{\min} < 10$ cm; $\mathrm{APD} = 0.3$ s, and for the normal CV without stretch $\mathrm{CV} = 70$ cm/s. Then the heart is vulnerable against regime **I** ($\mathrm{CV}_s = 70$ cm/s) for wave break, only if $T < 0.44$ s–10 cm/CV_f, and thus for a rapid heartbeat (faster than 136 bpm). For a release of external mechanical load (regime **II**) we predict that the heart is vulnerable ($\mathrm{CV}_f = 70$ cm/s), only if $T < 10$ cm/$\mathrm{CV}_s + 0.16$ s. For a heart rate of 60 bpm we expect that the heart is vulnerable if stretch slowed down waves to less than 11.9 cm/s before a stretch release and for 120 bpm to less than 30 cm/s.

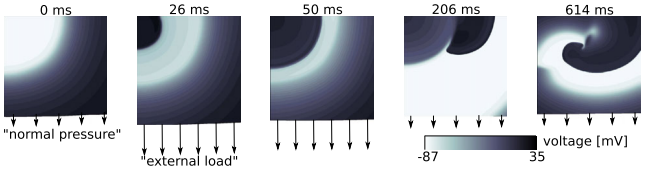

FIG. 5. Pulse of external mechanical load causes wave formation and break via regime **I**. Setup similar to Fig. 1 was used, but waves were started in the upper, left corner with a longer period of 500 ms. Stretch is applied at time 7450 ms with strength 24.0 kPa and duration 25 ms.

The mechanism may be studied experimentally in excised cardiac tissue slices [47,48], cell cultures [49], or animal models [50]. It may be interesting to affect CV by other means, e.g., with the optogenetics approach [51], to measure normal and critical CV in different cell types [compare Fig. 3(d)].

L. D. W. thanks the Deutsche Forschungsgemeinschaft for a research fellowship (Grant No. WE 5519/1-1). We thank Dr. Vadim Biktashev and Dr. Ivan Kazbanov for valuable discussions. We thank Dr. Hans Dierckx and Dr. Paul Baron for critical comments on the manuscript.

[1] B. P. Belousov, *Collection of Short papers on Radiation Medicine for 1958* (Med. Publ., Moscow, 1959), pp. 145–147, in Russian.
[2] A. Zaikin and A. Zhabotinsky, Nature (London) **225**, 535 (1970).
[3] N. Gorelova and J. Bures, J. Neurobiol. **14**, 353 (1983).
[4] G. Gerisch, W. Roux' Archiv Entwicklungsmechanik **156**, 127 (1965).
[5] C. Weijer, Curr. Opin. Genet. Dev. **14**, 392 (2004).
[6] A. Winfree and S. Strogatz, Nature (London) **311**, 611 (1984).
[7] D. Bers, *Excitation-Contraction Coupling and Cardiac Excitation Force*, 3rd ed. (Kluwer Academic Publishers, Dordrecht, Netherlands, 2001).
[8] P. Kohl, A. D. Nesbitt, P. J. Cooper, and M. Lei, Cardiovasc. Res. **50**, 280 (2001).
[9] P. Kohl, P. Hunter, and D. Noble, Prog. Biophys. Molec. Biol. **71**, 91 (1999).
[10] M. Nash and A. Panfilov, Prog. Biophys. Molec. Biol. **85**, 501 (2004).
[11] A. V. Panfilov, R. H. Keldermann, and M. P. Nash, Phys. Rev. Lett. **95**, 258104 (2005).
[12] L. D. Weise, M. P. Nash, and A. V. Panfilov, PLoS One **6**, e21934 (2011).
[13] L. D. Weise and A. V. Panfilov, PLoS One **8**, e59317 (2013).
[14] V. N. Biktashev, Phys. Rev. Lett. **89**, 168102 (2002).
[15] K. Ten Tusscher and A. Panfilov, Am. J. Physiol. Heart Circ. Physiol. **291**, H1088 (2006).
[16] S. Niederer, P. Hunter, and N. Smith, Biophys. J. **90**, 1697 (2006).

[17] S. Niederer and N. Smith, Prog. Biophys. Molec. Biol. **96**, 90 (2008).
[18] R. H. Keldermann *et al.*, Am. J. Physiol. Heart Circ. Physiol. **299**, H134 (2010).
[19] A. Hodgkin and A. Huxley, J. Physiol. **117**, 500 (1952).
[20] Euler integration with space step $HX = 0.025$ cm and time step $HT = 0.02$ ms.
[21] L. Verlet, Phys. Rev. **159**, 98 (1967).
[22] We chose a larger Verlet integration step *mt* (here: 0.05; in [13]: 0.01), a stricter threshold of convergence *thr* (here: 0.75 μN; in [13]: 125 μN), and a smaller (dimensionless) damping-stiffness ratio parameter d/c (here: 5; in [13]: 30; stiffness $c = 1$ here and in [13]). See Supplemental Material at http://link.aps.org/supplemental/10.1103/PhysRevLett.119.108101 for a validation of parameter settings.
[23] P. Kohl, P. Hunter, and D. Noble, Prog. Biophys. Mol. Biol. **71**, 91 (1999).
[24] K. Skouibine, N. Trayanova, and P. Moore, Math. Biosci. **166**, 85 (2000).
[25] P. Kohl, K. Day, and D. Noble, Can. J. Cardiol. **14**, 111 (1998).
[26] J. N. Weiss, A. Garfinkel, H. S. Karagueuzian, Z. Qu, and P.-S. Chen, Circulation **99**, 2819 (1999).
[27] See Supplemental Material at http://link.aps.org/supplemental/10.1103/PhysRevLett.119.108101 for movies on regimes for mechanically caused wave break.
[28] See Supplemental Material at http://link.aps.org/supplemental/10.1103/PhysRevLett.119.108101 for data on the influence of wave velocities on external mechanical load in the 2D point source setup.
[29] M. Masé and F. Ravelli, in *Mechanically Gated Channels and their Regulation, Mechanosensitivity in Cells and Tissues*, edited by A. Kamkin and I. Lozinsky (Springer Science & Business Media, New York, 2012), Chap. 11, pp. 303–324.
[30] R. W. Mills, A. T. Wright, S. M. Narayan, and A. D. McCulloch, in *Cardiac Mechano-Electric Coupling and Arrhythmias*, edited by P. Kohl, F. Sachs, and M. R. Franz (Oxford University Press, Oxford, England, 2011), Chap. 25, pp. 180–184.
[31] T. G. McNary, K. Sohn, B. Taccardi, and F. B. Sachse, Prog. Biophys. Mol. Biol. **97**, 383 (2008).
[32] To compute CV of a wave arrival times of the wave front (when: $V > -30$ mV and $\dot{V} > 0$) at finite difference points 0.5 cm apart were recorded.
[33] M. R. Franz *et al.*, Circulation **86**, 968 (1992).
[34] A. Panfilov, R. Keldermann, and M. Nash, Proc. Natl. Acad. Sci. U.S.A. **104**, 7922 (2007).
[35] J. J. Tyson and J. P. Keener, Physica D (Amsterdam) **32**, 327 (1988).
[36] I. Biktasheva, V. N. Biktashev, W. N. Dawes, A. V. Holden, R. C. Saumarez, and A. M. Savill, Int. J. Bifurcation Chaos Appl. Sci. Eng. **13**, 3645 (2003).
[37] R. D. Simitev and V. N. Biktashev, Biophys. J. **90**, 2258 (2006).
[38] A. Hill, Proc. R. Soc. A **119**, 305 (1936).
[39] K. Ten Tusscher, D. Noble, P. Noble, and A. Panfilov, Am. J. Physiol. Heart Circ. Physiol. **286**, H1573 (2004).
[40] M. G. Chang *et al.*, Heart Rhythm **9**, 115 (2012).
[41] N. Vandersickel, I. V. Kazbanov, A. Nuitermans, L. D. Weise, R. Pandit, and A. V. Panfilov, PLoS One **9**, e84595 (2014).
[42] See Supplemental Material at http://link.aps.org/supplemental/10.1103/PhysRevLett.119.108101 for further explanation
[43] See Supplemental Material at http://link.aps.org/supplemental/10.1103/PhysRevLett.119.108101 for an illustration how we predict wave break using normal and critical CV.
[44] See Supplemental Material at http://link.aps.org/supplemental/10.1103/PhysRevLett.119.108101 for movies that illustrate regimes of spiral wave annihilation.
[45] See Supplemental Material at http://link.aps.org/supplemental/10.1103/PhysRevLett.119.108101 for a movie that illustrates wave formation and wave break via regime **I** due to strong stretch.
[46] See Supplemental Material at http://link.aps.org/supplemental/10.1103/PhysRevLett.119.108101 for a derivation.
[47] K. Wang *et al.*, Prog. Biophys. Molec. Biol. **115**, 314 (2014).
[48] T. P. de Boer, P. Camelliti, U. Ravens, and P. Kohl, Future Cardiol. **5**, 425 (2009).
[49] Y. Zhang, R. B. Sekar, A. D. McCulloch, and L. Tung, Prog. Biophys. Molec. Biol. **97**, 367 (2008).
[50] M. S. Link *et al.*, N. Engl. J. Med. **338**, 1805 (1998).
[51] N. Magome, G. Kanaporis, N. Moisan, K. Tanaka, and K. Agladze, Tissue Eng. Part A **17**, 2703 (2011).